Available online at www.sciencedirect.com
ScienceDirect
International Journal of Mass Spectrometry 268 (2007) 106–121
International Journal of Mass Spectrometry
www.elsevier.com/locate/ijms

Resonant electron capture by some amino acids esters

Yury V. Vasil'ev [a,b,*], Benjamin J. Figard [c], Douglas F. Barofsky [a], Max L. Deinzer [a,c,*]

[a] Department of Chemistry, Oregon State University, Corvallis, OR 97331, United States
[b] Department of Physics, Bashkir State Agricultural University, Ufa, Russia
[c] Department of Biochemistry and Biophysics, Oregon State University, Corvallis, OR 97331, United States

Received 8 March 2007; received in revised form 12 July 2007; accepted 16 July 2007
Available online 22 July 2007

Dedicated to Professor Peter Roepstorff on the occasion of his 65th birthday.

Abstract

Resonant electron capture by Gly, Ala and Phe esters have shown that the most efficient negative ion (NI) fragmentations are associated with the C-termini. A new mechanism for the negative ion-forming processes at energies lower than those associated with the π^*_{OO} shape resonance involves coupling between dipole-bound and valence negative ion states of the same symmetry for amino acid conformers with high permanent dipoles. The interaction avoids crossing of the NI states and instead leads to formation of two adiabatic potential energy surfaces. Underivatized amino acids most effectively fragment from the bottom adiabatic surface via generation of $[M-H]^-$ carboxylate anions by hydrogen-atom tunneling through the barrier; fragmentation of the their esters with formation of analogues $[M-X]^-$ NIs occurs through the upper adiabatic state without penetration of the barrier in which the energy of the valence σ*(OX) resonance exceeds the bond dissociation energy of the neutral molecule. Low and high temperature resonant electron capture experiments point to the importance of conformational preferences of the amino acids for optimum dissociation of the parent NIs in the gas phase.

Keywords: Resonant electron capture mass spectrometry; Negative ion; Amino acid; Esterification

1. Introduction

Low-energy gas phase resonant reactions of free electrons and biologically relevant molecules that result in the generation of negatively charged species have attracted a great deal of interest in the last several years [1]. This notwithstanding, similar investigations of amino acids and peptides are still not very intensively studied subjects. In fact, only resonant electron capture by glycine [2–4], alanine [5], cysteine [6], proline [7], tryptophan [8], *N*-acetyl tryptophan [9], and valine [10] has been reported in an effort to elucidate the general tendencies of these elementary gas phase reactions. The main problem with such investigations is that it is difficult to introduce peptides and amino acids into the gas phase without them thermally breaking down during volatilization. Esterification of amino acids is a well-established method [11] for overcoming the volatility problems associated with the parent compounds. Based on previous efforts [12,13] to study resonant electron capture of some amino acids and their methyl (Me) esters, we have performed additional studies with ethyl (Et), isopropyl (*i*-Pr), and *t*-butyl (*t*-Bu) esters of glycine (Gly), alanine (Ala), and phenylalanine (Phe). These experiments have been conducted to shed more light on the effects that esterification of the amino acids have on negative ion (NI) formation and decay mechanisms resulting from low-energy resonant electron capture. Another important issue has been the possible changes of the relative populations of different conformers of the amino acids in the gas phase due to esterification. This question has previously been considered in the case of Gly conformers [14]. Resonant electron capture mass spectrometry was used in the present work to probe the question further since this method has proven to be a very sensitive and powerful tool with respect to the change of both geometric and electronic structures of the compounds under study. Moreover, conformers of the simplest amino acid, Gly, are known to possess different magnitudes and directions of their dipole moments within the molecular framework [15]; other amino acids, having structures

* Corresponding authors at: Department of Chemistry, Oregon State University, Corvallis, OR 97331, United States.
E-mail addresses: Y.Vasilev@orst.edu (Y.V. Vasil'ev), Max.Deinzer@oregonstate.edu (M.L. Deinzer).

1387-3806/$ – see front matter © 2007 Elsevier B.V. All rights reserved.
doi:10.1016/j.ijms.2007.07.006

that are even more complex are supposed to possess similar features. Such molecular species having dipole moments larger than the critical magnitudes (2–2.5 D [16,17]) are able to create so-called dipole-bound or dipole-supported NIs that are different from "chemical" or valence NI states. Dipole-bound NIs were very intensively studied both theoretically and experimentally and recently [18] the topic gained added significance in light of the interactions of valence and dipole-supported anion states and the influence on NI fragmentation channels of the combined NI states in DNA and RNA bases. Experimental proof for the existence of such species in Gly–water clusters [19] and even bare Gly molecules [20] have also been reported. The present analysis of $[M-H]^-$ NI formation in amino acids via resonant electron capture at 1.2–1.3 eV showed that these ions have both appearance energies and peak maxima that are lower than the putative thresholds and resonance centers associated with the π^*_{OO} "acidic orbitals" as determined from electron transmission spectra [21]. That means that π^*_{OO} shape resonances cannot be considered as the parent states for the generation of $[M-H]^-$ fragment NIS as considered earlier [3–10,12], at least not for the energy range in which the electron transmission and resonant electron capture data do not match. Questions concerning the real mechanism of $[M-H]^-$ NI production, i.e., how the π^*_{OO} orbital fits into the picture, and whether dipole-bound NI states are involved in the mechanism need to be answered. A variation in the spatial requirements and masses of departing neutral particles that result in the formation of carboxylate anions via resonant electron capture by different amino acid esters has been used in the present work to shed some light on these questions.

2. Computational methods

The starting geometry of the amino acids and their esters was based on results from semi-empirical calculations at the PM3 level of theory. The data were further used for calculations of the electronic and geometric structures of neutral molecules and their molecular and fragment NIs using Hartree–Fock SCF (6-31G*) theory. PM3 calculations also were used for the estimations of some resonant electron capture reaction enthalpies.

3. Experimental

A custom-made [22] gas chromatograph/resonant electron capture-TOF mass spectrometer incorporating a trochoidal electron monochromator (electron current 5–100 nA; energy spread 60–200 meV, FWHM, energy from 0 to 12 eV) was used for the study of resonant electron attachment reactions of Gly, Ala, and Phe methyl (Me), ethyl (Et), isopropyl (*i*-Pr), and *t*-butyl (*t*-Bu) esters. Samples of amino acids and their esters were initially loaded into two glass capillaries that were inserted one inside the other in order to prevent contact with the metal walls of the inlet system and thus to eliminate or minimize thermal degradation of the compounds. The capillaries were then placed into a homemade direct insertion probe that was inserted into the ionization chamber through a vapor lock. The ionization chamber and direct insertion probe were heated separately. Since the results from previous experiments with amino acids and their esters were reported [12], the instrument underwent modifications to increase its sensitivity that allowed for confident ion signal registration with lower temperatures in both the inlet system and the ionization chamber. The ionization chamber was kept at ca. 40–120 °C to prevent possible influence from ambient conditions. The temperature of the inlet system was set depending on the compound studied: 140 °C (Gly), 125 °C (Ala), 180 °C (Phe), whereas the temperatures for the esters ranged from 90 to 120 °C depending on their sizes. *i*-Pr esters of Gly and Phe were available in limited amounts and their resonant electron capture spectra were conducted only once at the same time as experiments in Ref. [12] and therefore at higher temperature conditions. The electron beam and sample vapor that effuse from the direct insertion probe interact in the ionization chamber. The NIs formed after electron attachment are drawn in a direction orthogonal to the electron beam and into the time-of-flight analyzer by an electric field created by application of a voltage with respect to the ionization chamber of ca. +15 V and <−0.1 eV to an extraction and a repeller electrode, respectively. The mass and energy scales were calibrated using CCl_4 and low pressure (<10^{-7} Torr) SF_6-gas. As in previous studies [12], CCl_4 was used only at the initial stage of the experiments with the esters; after achieving the inlet system temperature for effective sample vaporization, CCl_4 effusion was shut off and Cl^- from HCl associated with salts of the ester were used for further calibration. The pressure measured with an external ion gage near the ionization chamber did not exceed 5×10^{-6} Torr thereby providing single-collision conditions throughout the experiment.

Amino acids were purchased from Sigma–Aldrich Chemical Co. (St. Louis, MO) with stated purity of 99% or better. Amino acid esters also were purchased from Sigma–Aldrich (Milwaukee, WI) with stated purities of 98% or better. These compounds were used without further purification.

4. Results and discussion

All amino acid esters, from Me to *t*-Bu showed remarkable similarity in their resonant electron capture spectra. As previously observed for underivatized amino acids [12], none of them formed long-lived (lifetime exceeding microseconds) molecular NIs of the valence type in the explored energy range. However, in contrast to underivatized amino acids, none of the esters studied showed efficient formation of carboxylate anion, $[M-X]^-$ (X stands for Me, Et, *i*-Pr, or *t*-Bu) in the 1 eV region. This fact was also noted earlier [12] in the case of Me-esters of amino acids and the explanation offered at the time was related to the specificity of the ion formation mechanism in this energy range that involved tunneling through the energy barrier of the departing particle. For this reason, the vast majority of the ion formation processes in the amino acid esters studied occur at higher energies. Below, Gly, Ala, and Phe and their esters are considered separately in an effort to emphasize this similarity while at the same time showing some differences in the spectra when present. Only the most charac-

teristic and efficient ion fragmentation pathways for both the amino acids and their esters are discussed. For this reason, a discussion of lower mass NIs that were considered in detail previously [12] are omitted here because their origin often needs special proof which is beyond the main aim of the present work.

4.1. Glycine esters

To facilitate interpretation, ion production processes were normalized to the yield of OX^- NIs in the energy range 5.5–6 eV for all Gly-based compounds (Table 1). This was done because generation of the $[M-H]^-$ NIs in underivatized amino acids at 1.2–1.3 eV is the dominant ion-forming process and it was feared that taking it as a benchmark for the rest of the compounds could conceal the general spectral trend. Separate columns were also shown for all compounds with integrated yield, I_{int}, of a particular ion over the explored energy range, again in comparison to that of OX^- NIs (Table 1). All fragment NIs (Table 1) are associated with the C-terminus, except $[M-NH_2]^-$, the formation of which involves bond cleavage directly associated with the N-terminus. Complementary NH_2^- NIs are not considered here since they could be confused with other NIs of the same nominal mass, the origins of which were impossible to determine precisely in the course of the present work. As already mentioned, experiments with Gly *i*-Pr ester were conducted at higher temperatures of the ionization chamber and the inlet system and some results for this compound may deviate slightly from the trends found for the rest of the compounds.

In addition to the 5.5–6 eV energy range, OX^- NIs are also produced from two other resonances near 3 and 7 eV (Table 1). Relative intensities of these NIs from the low-energy resonance increase with size of the esters, whereas the yields of these ions near 7 eV vary only slightly relative to their peak magnitude at 5.5–6 eV. Complementary $[M-OX]^-$ ions displayed the same behavior in the energy range 5–5.6 eV, but yields were low and almost invariable. Interestingly, dissociation processes for the esters that supposedly occur via hydrogen-atom loss and elimination of the respective alcohol (water in underivatized amino acids [12]), $[M-H-HOX]^-$, proceed in the same energy range as that of the internal standard, OX^- NIs, and show almost no indication of a relative intensity change. $[M-H]^-$ NIs show behavior similar to OX^- ions in the energy range near 5.5 eV, but near 3 eV, their signals gradually lower as the substitution proceeds from Me to *t*-Bu ester. A reversed trend was observed for the $[M-NH_2]^-$ NIs. The ion intensities are practically constant for all four esters at 1.7–2 eV but decrease in intensity at 5–5.5 eV going from Me to *t*-Bu ester.

$[M-X]^-$ NIs were generated at nearly all of the resonant energies discussed above for the four esters studied and showed gradual increase in intensity at all resonances as substitution proceeded through the series from Me to *t*-Bu. Generation of these ions near 1 eV is the dominant process in dissociative electron capture spectra of underivatized amino acids [12]. Therefore, even very low amounts of amino acids present in the samples due to, for instance, incomplete esterification reaction is

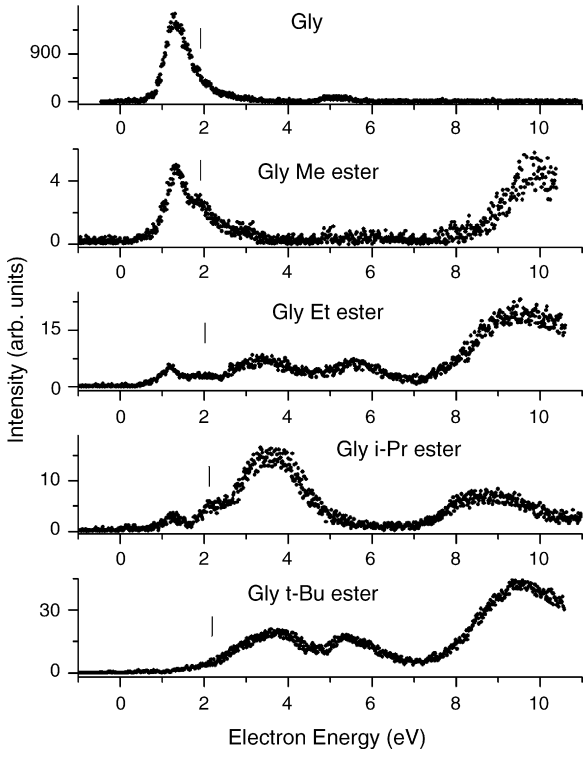

Fig. 1. Effective yield curves of $[M-X]^-$ NIs from Gly and its esters. The vertical bars indicate positions of π^*_{OO} shape resonances determined either from calculations (esters; see also Table 2) or taken from Ref. [21] (Gly).

expected to cause appearance of the ion signal near 1 eV from the underivatized compound; this possibility was noted previously [12]. Fortunately, esterified amino acids require lower temperatures to vaporize in comparison to the underivatized compounds and therefore, lower temperatures used in the present experiments resulted in much lower abundances of $[M-H]^-$ near 1 eV (Table 1). Another advantage of the low temperatures used is the observation of an additional resonance state near 2 eV that produces $[M-X]^-$ NIs, which were very difficult to discern in the earlier experiments [12], but are clearly apparent here (Fig. 1; Table 1).

Thus, from the preceding experimental analyses, it was observed that there were at least five energy ranges with NI resonances that decay into different fragment NIs. These were near 1 eV (I), 2 eV (II), 2.5–3.5 eV (III), 5.5–6 eV (IV), and higher 7 eV (V). Quantum chemical calculations on electronic and geometric structures of Gly-based compounds were used to help rationalize these observations.

It is now well established [14,15] that the most stable Gly conformer is I_p (Fig. 2; nomenclature by Császár [23] is used throughout this work for identification of the Gly conformers, where p stands for the structure that has planar, C_s, symmetry). According to the most sophisticated calculations [14,23] performed on Gly conformers, II_n, (n means that the structure is non-planar and has no element of symmetry) is the second stable structure of Gly and, depending on the level of theory, II_n is 0.5–3 kcal/mol higher in energy than I_p. The present calculations performed by HF 6-31G* theory (Fig. 2; Table 2) predict ener-

Table 1
Resonant electron capture mass spectra of glycine, $H_2NCH_2C(O)OX$, (X = H) and its methyl (X = Me), ethyl (X = Et), isopropyl (X = *i*-Pr), and *t*-butyl (X = *t*-Bu) esters

Ions	X = H			X = Me			X = Et			X = *i*-Pr[a]			X = *t*-Bu		
	m/z	*I*, % (E_m, eV)	I_{int}	*m/z*	*I*, % (E_m, eV)	I_{int}	*m/z*	*I*, % (E_m, eV)	I_{int}	*m/z*	*I*, % (E_m, eV)	I_{int}	*m/z*	*I*, % (E_m, eV)	I_{int}
$[M-H]^-$	74	128 (5.5)	142	88	13 (≈2.8) 25 (≈5.3)	16	102	3 (≈3) 19 (≈5.5)	12	116	2.5 (≈2.5–3)[b] 11 (5.2)	8	130	≈1.5 (≈2.5–3)[b] 37 (≈5.3)	27
$[M-X]^-$	74	2263 (1.28)	2756	74	10 (≈1.3)[c] 3 (1.8) <1 (2.5–3) sh. 11 (≈9.7)	11	74	10 (≈1.3)[c] 5 (≈2) sh. 19 (≈3.5) 15 (≈5.5) 39 (≈9.5)	69	74	8 (≈1.3)[c] 15 (≈2.1) sh. 95 (≈3.6)[d] 45 (≈8.5–9.5)[b]	200	74	10 (≈2) sh. 63 (3.6) 51 (5.4) 116 (9.5)	208
$[M-NH_2]^-$	59	10 (≈2) 9 (5.2)	11	73	≈2.5 (≈2) ≈7.7 (5)	5.9	87	2 (≈1.7) 2 (≈5.5)	1.7	101	7 (≈1.6) 4.5 (≈5)	5.4	115	3.5 (≈1.7) 1.5 (≈5.5)	1.5
$[M-OX]^-$	58	9 (1.5)[e] 13 (5)	10	58	≈3.8 (≈5.6) 21 (≈7.6) 9.2 (≈9)	21	58	2.3 (5.5)	3	58	4.5 (≈5)	4.6	58	≈5 (5.2)	4.8
$[M-H-HOX]^-$	56	61 (5.5)	37	56	58 (≈5.9)	39	56	35 (≈6.3)	37	556	60 (≈5.5)	62	56	58 (≈5.9)	65
$COOX^-$	45	6 (2.8) 175 (5.6)	91	59	164 (5.6) 33 (≈7.5)	111	73	41 (≈5.7)	28	87	11 (≈5.5) 4.5 (≈7)	9.2	101	1.5 (≈5.5)	2.5
OX^-	17	100 (6) 44 (10)	100	31	≈1.5 (≈3) 100 (≈5.9) 50 (≈7.4)	100	45	2.3 (≈3.3) 100 (≈5.9) 37 (≈7) sh.	100	59	9 (≈3) 100 (≈5.5)	100	73	9 (≈2.8) 100 (≈5.6) 45 (≈7) sh.	100

[a] Experimental conditions similar to that of Ref. [12] (high temperature) have been used to record spectra of this compound.
[b] Precise determination of resonance maxima was impossible.
[c] The ions at low (1.2–1.3 eV) energy are supposed to be $[M-H]^-$ ions from underivatized glycine that may be present as an impurity.
[d] The effective yield curve of these ions is very wide and determinations of possible contributions from resonance states near 5.5 eV not possible.
[e] Comparison with C_α-D_2–Gly showed that these NIs at 1.7 eV are more likely $[M-NH_3]^-$ than $[M-OX]^-$.

Table 2
Results of quantum chemical calculations of conformers of Gly (X = H) and its esters (X = Me, Et, *i*-Pr, and *t*-Bu) on the base of HF 6-31G* level of theory; E_{rel} is the total energy for different conformers with respect to that of I_p conformer; μ dipole moment; $E[\pi^*_{OO}]$, $E[\sigma^*_{OX}]$, $E[\sigma^*_{C-OX}]$, $E[\sigma^*_{C_\alpha-H}]$, $E[\sigma^*_{C_\alpha-N}]$, $E[\sigma^*_{N-H}]$ are energies of corresponding vacant molecular orbitals scaled according to equations from Ref. [21] (π^* orbitals) and from Ref. [18] (σ^* orbitals; scaling on the base of Ref. [21] is given for σ^* orbitals in brackets for comparison)[a]

	Conformers				
	I_p	II_n	III_p	IV_n	V_n
X = H					
E_{rel} (kcal/mol)	0	2.93	1.91	2.07	3.06
μ (D)	1.3	5.69	2.04	2.3	2.74
$E[\pi^*_{OO}]$ (eV)	1.897	1.703	1.863	1.912	1.863
$E[\sigma^*_{OX}]$ (eV)	2.97 (2.6)	4.59 (3.91)	2.6 (2.31)	3.04 (2.66)	2.83 (2.49)
$E[\sigma^*_{C-OX}]$ (eV)	6.09 (5.12)	6.78 (5.68)	6.12 (5.15)	7.43 (6.3)	7.51 (6.27)
$E[\sigma^*_{C_\alpha-H}]$ (eV)	4.34 (3.71)	3.93 (3.38)	4.29 (3.67)	4.34 (3.71)	4.38 (3.74)
$E[\sigma^*_{C_\alpha-N}]$ (eV)	4.71 (4.0)	5.92 (4.99)	4.64 (3.95)	5.25 (4.44)	4.67 (3.98)
$E[\sigma^*_{N-H}]$ (eV)	3.05 (2.67)	2.6 (2.31)	3.45 (2.99)	3.2 (2.79)	3.65 (3.15)
	Conformers				
	I_p	II_n[b]	III_p	IV_n	V_n
X = Me					
E_{rel} (kcal/mol)	0	11.87	1.91	2.03	2.97
μ (D)	1.92	4.74	2.55	2.4	2.83
$E[\pi^*_{OO}]$ (eV)	1.973	1.593	1.93	1.981	1.95
$E[\sigma^*_{OX}]$ (eV)	3.8 (3.27)	3.04 (2.66)	3.72 (3.21)	3.84 (3.3)	3.79 (3.26)
$E[\sigma^*_{C-OX}]$ (eV)	6.36 (5.34)	6.12 (5.15)	6.26 (5.26)	5.94 (5.0)	5.96 (5.01)
$E[\sigma^*_{C_\alpha-H}]$ (eV)	4.34 (3.71)	4.48 (3.82)	4.35 (3.72)	4.33 (3.7)	4.47 (3.81)
$E[\sigma^*_{C_\alpha-N}]$ (eV)	4.75 (4.04)	4.68 (3.98)	4.71 (4.0)	4.91 (4.17)	4.77 (4.06)
$E[\sigma^*_{N-H}]$ (eV)	3.05 (2.67)	3.71 (3.2)	2.93 (2.57)	3.25 (2.83)	3.24 (2.82)
X = Et					
E_{rel} (kcal/mol)	0	12.67	1.93	2.03	2.97
μ (D)	2.09	4.72	2.73	2.52	2.93
$E[\pi^*_{OO}]$ (eV)	2.01	1.61	1.97	2.01	1.98
$E[\sigma^*_{OX}]$ (eV)	3.42 (2.96)	3.76 (3.24)	3.38 (2.93)	3.46 (3.0)	3.43 (2.97)
$E[\sigma^*_{C-OX}]$ (eV)	6.42 (5.39)	6.32 (5.31)	6.34 (5.32)	6.13 (5.16)	5.57 (4.7)
$E[\sigma^*_{C_\alpha-H}]$ (eV)	4.36 (3.73)	4.63 (3.95)	4.26 (3.65)	4.36 (3.73)	4.35 (3.72)
$E[\sigma^*_{C_\alpha-N}]$ (eV)	4.69 (3.99)	5.09 (4.32)	4.59 (3.91)	5.36 (4.53)	4.83 (4.11)
$E[\sigma^*_{N-H}]$ (eV)	3.05 (2.67)	3.17 (2.77)	2.9 (2.55)	3.24 (2.82)	3.24 (2.82)
X = *i*-Pr					
E_{rel} (kcal/mol)	0	14.62	2.0	2.04	2.96
μ (D)	2.12	4.82	2.69	2.38	2.74
$E[\pi^*_{OO}]$ (eV)	1.999	1.897	1.968	2.0	1.97
$E[\sigma^*_{OX}]$ (eV)	3.37 (2.93)	2.64 (2.33)	3.3 (2.87)	3.1 (2.71)	3.15 (2.75)
$E[\sigma^*_{C-OX}]$ (eV)	6.38 (5.36)	6.2 (5.21)	6.36 (5.34)	6.44 (5.4)	6.46 (5.42)
$E[\sigma^*_{C_\alpha-H}]$ (eV)	4.46 (3.81)	4.76 (4.05)	4.35 (3.72)	4.48 (3.82)	4.42 (3.77)
$E[\sigma^*_{C_\alpha-N}]$ (eV)	4.8 (4.08)	5.37 (4.54)	4.68 (3.99)	5.21 (4.41)	4.8 (4.08)
$E[\sigma^*_{N-H}]$ (eV)	2.98 (2.61)	3.2 (2.79)	2.9 (2.55)	3.49 (3.02)	3.43 (2.97)
X = *t*-Bu					
E_{rel} (kcal/mol)	0	14.92	2.04	2.05	2.97
μ (D)	2.2	4.64	2.8	2.47	2.82
$E[\pi^*_{OO}]$ (eV)	2.028	1.89	1.999	2.03	1.993
$E[\sigma^*_{OX}]$ (eV)	3.82 (3.29)	2.56 (2.27)	3.28 (2.86)	2.91 (2.55)	2.9 (2.55)
$E[\sigma^*_{C-OX}]$ (eV)	6.2 (5.21)	6.87 (5.75)	6.27 (5.27)	6.86 (5.75)	6.94 (5.81)
$E[\sigma^*_{C_\alpha-H}]$ (eV)	4.47 (3.815)	4.37 (3.74)	4.396 (3.76)	4.47 (3.82)	4.4 (3.76)
$E[\sigma^*_{C_\alpha-N}]$ (eV)	4.94 (4.19)	5.31 (4.49)	5.04 (4.27)	5.43 (4.59)	5.4 (4.57)
$E[\sigma^*_{N-H}]$ (eV)	3.29 (2.86)	3.22 (2.81)	2.65 (2.35)	3.42 (2.97)	3.41 (2.96)

[a] Energies of these normally unoccupied π^* and σ^* orbitals can be associated with energy maxima of corresponding shape resonances via a scaling procedure, however, these negative ion states are temporary states (resonances) and the resonance widths, another important characteristics of the resonances, cannot be determined from these calculations.

[b] Because of the non-planar structures, many orbitals mutually mixed and it was difficult to identify some of them.

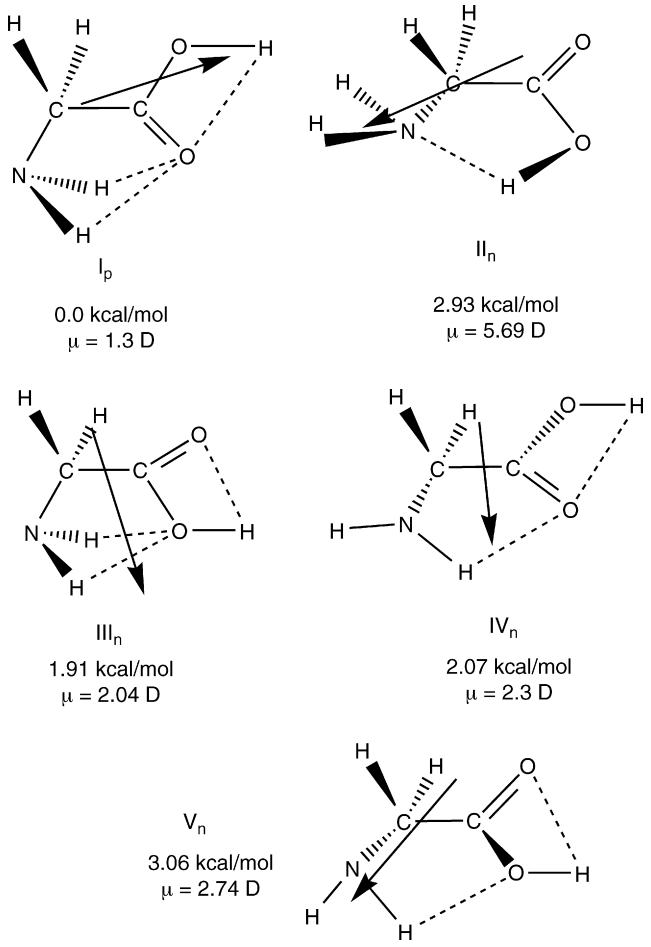

Fig. 2. Five of the most stable conformers of Gly determined on the basis of HF 6-31G* level of theory. Energies of the conformers are given in relation to the most stable conformer I_p. Dipole moments (directions within the molecular frame are represented by arrows) are given in Debyes (D).

gies for three other conformers of Gly, III_p, IV_n, and V_n that are relatively close to these results [14,23] except for the fact that the III_p and IV_n conformers are predicted to be more stable in comparison to the II_n. This controversy concerning 6-31G* based-results is known and rather well understood [14]. Using the same 6-31G* level of theory, the dipole moments for the Gly conformers were calculated and compared with published data for the I_p and II_n conformers [15] that were based on a higher level of theory. Comparisons showed very good agreement with the known data for I_p and II_n. Császár's [23] calculations based on MP2 level of theory predicted the following mole fractions for the Gly confomers in the gas phase at 473 K: 71.1, 12.5, 3.4, 9.9, 2.8% for I_p, II_n, III_p, IV_n, V_n, respectively. Nguyen et al. [14], using ACM/DZVP theory, predicted gas phase concentrations for these conformers to be 62.1, 12.3, 10.0, 11.4, and 3.3%, respectively. Since temperatures in our experiments were lower than 473 K, the gas phase mole fraction of the I_p conformer could probably be even larger in comparison to other conformers than would be expected from these theoretical predictions. However, although the mole fraction of II_n is lower in comparison to I_p under conditions of the present experiments, the higher dipole moment of II_n can in principle enhance electron attachment cross-section and the ions originating from the II_n conformer can have comparable or even higher signals than that arising from I_p. It is also important to note that directions of the permanent dipoles in these two conformers are practically opposite to one another (Fig. 2) and therefore, dipole-bound anions will interact more effectively with different NI valence states of Gly. As noted by Gutowski et al. [15], only the dipole moment of the IIn conformer is able to create a bound NI state, whereas the dipole moment of I_p does not exceed the critical value ≈2–2.5 D [16,17]. According to the present calculations, dipole moments of the III_p, IV_n, and V_n conformers are also close to the critical value, however, only gas phase concentrations of the III_p and IV_n conformers according to Nguyen et al. [14] could contribute to resonant electron capture at the temperatures used in the present experiments.

As mentioned above, a direct comparison of $[M-H]^-$ effective yield curve from Gly resonant electron capture spectrum with Gly electron transmission spectrum, i.e., with the total electron attachment cross-section, raises doubts about the earlier suggested mechanism that a π^*_{OO} shape resonance decays into $[M-H]^-$ NIs, at least at electron energies <1.5 eV. The shapes of these π^*_{OO} "acidic orbitals" (Fig. 3; Table 2) were found to be practically identical both for conformers of underivatized Gly and that of its esters, whereas the energies of the orbitals vary slightly depending on the conformers and esterifying alkyl groups. Since the π^*_{OO} shape resonance is the lowest possible valence NI state within the Franck–Condon region of a neutral molecule for all conformers of Gly that could be present in the gas phase at the temperatures used in the present experiments, the origin of these $[M-H]^-$ NIs is not associated with the valence type NIs at energies lower than 1.5 eV. This is remarkable because these ions, not directly originating from valence type resonances, possess the highest yield over the entire energy range for all underivatized amino acids studied thus far. It was suggested earlier [12] that the amino acid NIs could be associated with the generation of dipole-supported NIs under low-pressure plasma conditions [24]. Photoelectron spectroscopy of negatively charged Gly [20] unambiguously proved the existence of these types of ions and the authors associated them with the II_n conformer of Gly. An unusual vibrational structure that was identical with the infrared vibration of neutral II_n Gly conformer was observed in the photoelectron spectrum [20]. Since the positive end of the dipole is located proximate to the amino-group of the II_n conformer (Fig. 2), it was very surprising to observe excitation of the OH-stretching mode. However, a red-shift of the OH-stretching mode in comparison to the free OH-group was certainly indicative of intramolecular hydrogen bonding (Fig. 2) between the amino-group nitrogen and the hydroxyl-hydrogen [25]. In another words, a dipole-supported state of II_n can interact with the valence σ*(OH) state because of this internal hydrogen bond. This interaction precludes crossing of the two states and creates a barrier through which a hydrogen atom from the OH-group can tunnel (Fig. 4A) analogous to that proposed for DNA and RNA bases [18] and other OH-group containing molecules [26]. Märk and coworkers who used the highest electron energy resolving power known thus far to inves-

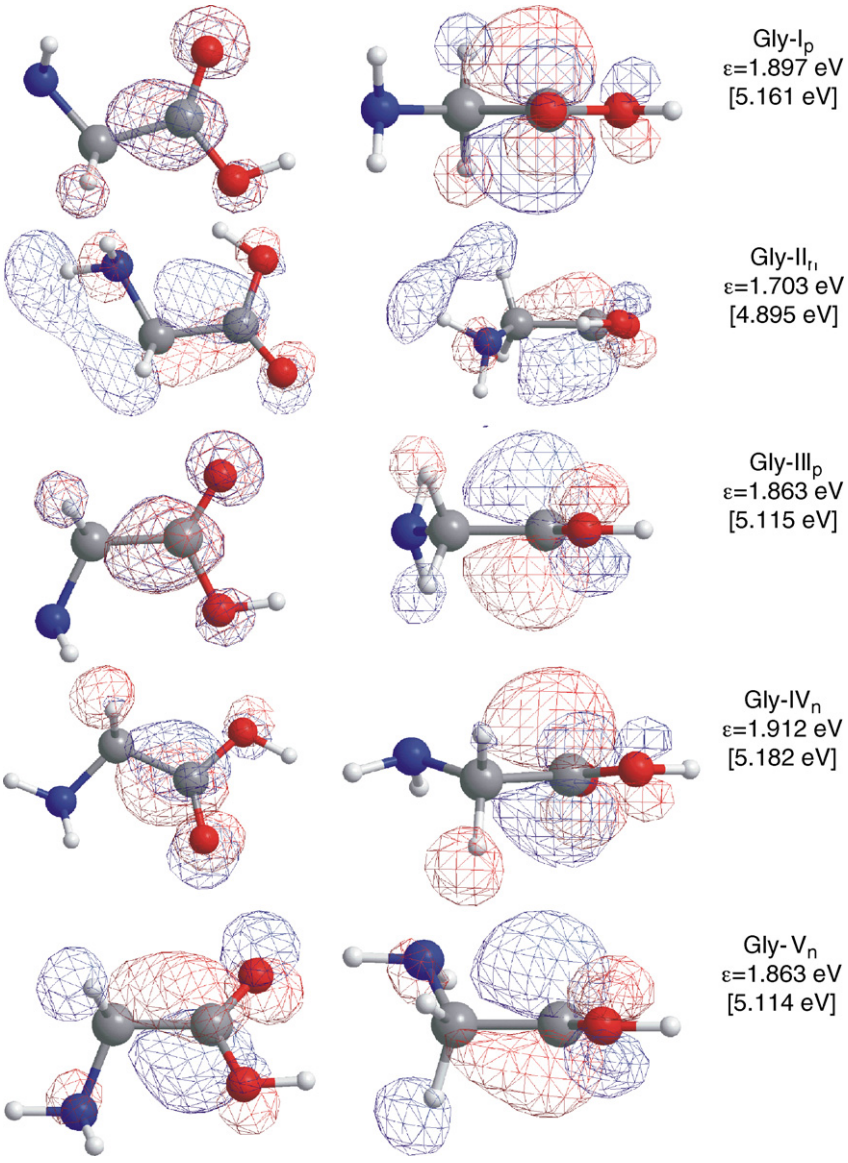

Fig. 3. π^*_{OO} "acidic orbital" for five main Gly conformers in two projections determined on the basis of HF 6-31G* level of theory. Energies of the orbitals have been scaled according to the equation derived in Ref. [21]; unscaled orbital energies are indicated in brackets.

tigate NIs of amino acids, observed vibrational fine structure in the $[M-H]^-$ effective yield curve of Gly [4] and Ala [5]. Although not very well resolved, the vibrational fine structure, indicative of vibrational Feshbach resonances, was certainly evident as shoulders in the effective yield curves of these $[M-H]^-$ NIs. Moreover, based on the calculated heats of formation for these reactions, appearance energies for the $[M-H]^-$ NIs are 1.094 eV for the II_n conformer and 1.235 eV for the I_p conformer. The experimental appearance energy value 1.10 ± 0.05 eV [12] matches that for the II_n conformer better than for I_p. The formation of $[M-H]^-$ NIs associated with the loss of hydrogen atoms from Gly in the energy range 1.2–1.3 eV [12] cannot occur from anywhere else except the OH group. Overall the results, point to the decisive role of the dipole-bound NIs in the Gly II_n conformer for the production of $[M-H]^-$ NIs at energies <1.5 eV. Participation of the earlier suggested π^*_{OO} shape resonance in the effective yield curve of $[M-H]^-$ probably starts at energies >1.5 eV. However, even in this case interaction via vibrations with the repulsive σ*(OH) state is required to complete the fragmentation and in principle it can occur for all Gly conformers (Fig. 4) if they are present in the gas phase under conditions of the present experiments. The π^*_{OO} shape resonance in this case serves as a "doorway" state [18] for the fragmentation and in this sense it is analogous to the above discussed dipole-bound NI state. For underivatized Gly, this process is difficult to recognize because the resonance is hidden by much more intense fragmentations associated with the dipole-bound NI state. The tunneling mechanism cannot occur for esters (Fig. 4D) because of the heavier masses of the departing alkyl radical, which results in much clearer π^*_{OO} shape resonance peaks associated with fragmentations in the effective yield curves for $[M-X]^-$ NIs near ca. 2 eV (Fig. 1, Table 1).

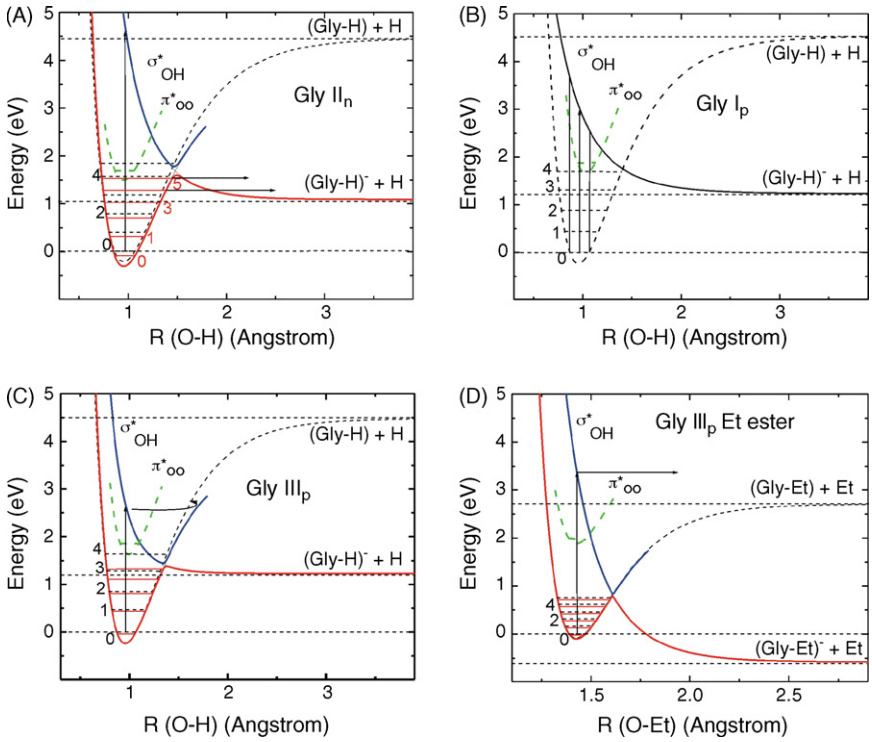

Fig. 4. Cut through the potential energy surface of the Gly II_n (A), I_p (B), III_p (C), and Gly Et ester III_p (D) conformers along the O–H stretching mode. The neutral molecule curves and their vibrational levels are shown as dashed lines; the dipole-bound and σ^*_{OH} NI diabatic states as solid lines; the adiabatic states as colored solid lines (bottom state in red and upper state in blue); π^*_{OO} state as green short dashed line. The vertical arrows show energy transitions from the neutral molecule to the σ^*_{OH} state; two horizontal arrows in A indicate positions of the vibrational Feshbach resonances (see Fig. 5 and Ref. [4]); dashed horizontal lines show [M−H] bond dissociation energies (BDE) of neutral molecules (upper line), $[M-X]^-$ NI appearance energies (AE, middle lines for A–C, and bottom line for D), and zero-point energy level for the neutral molecule. The curves have been calculated using Morse potentials (bound states) and anti-Morse potentials (repulsive states) on the basis of calculated or literature data of the shape resonance energies, appearance energies, BDEs, AE, electron affinities, vibrational energies (second order of unharmonicity was included). Perturbation theory was used to calculate the avoided crossing model and the off diagonal coupling element has been taken close to the energy difference between the neutral molecule and the dipole-bound NI states at relaxed geometries.

However, even in this case, the lower energy range overlaps with possible contributions from underivatized Gly that may be present. This situation is somewhat similar to two processes that produce $[M-H]^-$ NIs from acetic acid in which less intensive fragmentations became ill-defined in the presence of the much more abundant dissociation of the OH-bond, which, incidentally, was also accompanied by excitation of the ν(OH) stretch [2].

Additional experiments to support the hypothesis described here have been carried out using high-energy resolving power. The energy spread of the electron beam before introducing the Gly sample into the instrument was ca. 60 meV and during the experiments the energy spread gradually increased to 100–110 meV. These experimental results have been carefully analyzed via the Voigt function fitting procedure (Fig. 5). Voigt function fitting showed that the effective yield curve of $[M-H]^-$ NIs consists of three resonance peaks, two of which are believed to be vibrational Feshbach resonances (blue curves in Fig. 5) and the third, a π^*_{OO} shape resonance (green curve).

$[M-NH_2]^-$ NIs were also observed from a resonance state near 2 eV (Table 1). It is assumed that the π^*_{OO} shape resonance proceeds via π orbital electron capture followed by orbital mixing with the neighboring σ^*_{N-H} state (Table 2) through excitation

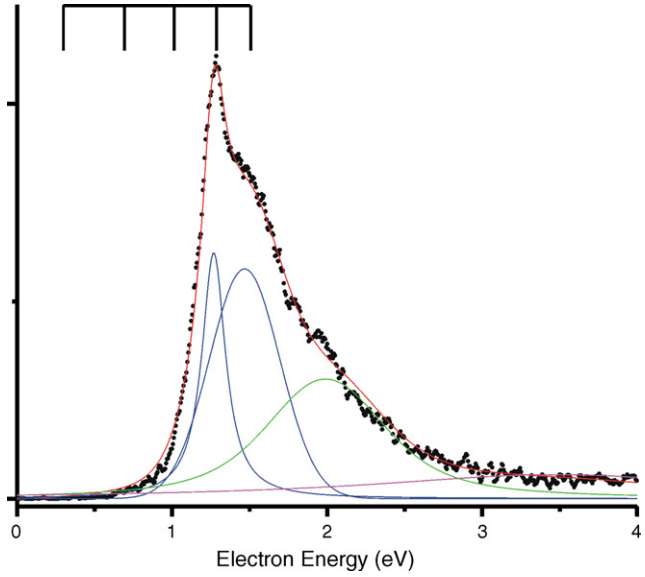

Fig. 5. Effective yield curve of $[M-H]^-$ negative ions for Gly recorded with high energy-resolving power and deconvolution by Voigt function peak fitting (two blue curves are vibrationally excited Feshbach resonances decaying via tunneling into $[M-H]^-$ NIs and correspond to two horizontal arrows in Fig. 4(A); the green curve is the contribution from a π^* shape resonances; the magenta curve is background and the red curve is the sum of these four curves).

of appropriate symmetry vibrational modes. The σ^*_{N-H} state is repulsive along C_α–N bond and as a result, $[M-NH_2]^-$ are formed. Since only π^*_{OO} orbitals of Gly conformers with non-planar structures have significant contribution at the NH_2-group, it is reasonable to conclude that these ions are predominantly formed from the conformers. Indeed, because of the higher temperatures that must result in a higher mole fraction of non-planar conformers for the *i*-Pr ester, an increase in the cross-section of the NIs near 2 eV was observed compared to the other esters studied at lower temperatures.

In the case of formic acid, Allan [27], who investigated vibrational excitations in the electron impact experiments, discussed possible direct electron capture into the σ*(OH) orbital resulting in a shape resonance, which being very broad could affect vibrational excitations at energies well below that of the nominal energy of the resonance. The σ* shape resonances of compounds consisting of second row-elements have very short lifetimes making them very difficult to isolate and identify experimentally [21]. In principle, the mechanism [27] can be realized during generation of $[M-H]^-$ NIs in Gly and very fast electron autodetachment at higher energies could be responsible for the formation of a much narrower (compared to the parent σ* resonance) resonance-like shapes of the effective yield curves of $[M-H]^-$ NIs with maxima at 1.2–1.3 eV. However, there are issues that cast doubt on such a fragmentation mechanism for Gly and its esters. If it were the case, the yield curves of $[M-H]^-$ NIs from Gly and $[M-X]^-$ NIs from esters should be identical because the calculated energies for the σ*(OX) orbitals (Table 2) varied less than 1 eV around the mean value of 3.5 eV. Instead, dramatic differences in the shapes of the effective yield curves for $[M-X]^-$ NIs of esters and underivatized Gly have been observed. The $[M-X]^-$ NIs effective yield curves from the *t*-Bu ester (Fig. 1) showed no resonance peaks at 1.2–1.3 eV since this ester sample contained less underivatized Gly than did the samples of other Gly esters. It is also noted that the σ*(OX) orbital energy of the II_n conformers deviates more than 1 eV about the mean of 3.5 eV (Table 2). Such deviations are caused by changes in conformers upon esterification that result in large increases in both the total and the orbital energies (Table 2). Because of their high total energy, these Gly ester conformers should not be present in the gas phase in any significant amount, at least not under the conditions of the present experiments.

In the energy range ∼3–3.5 eV where $[M-H]^-$, $[M-X]^-$, and OX^- NIs were observed, it is unclear whether there is just one or several superimposed resonances each possessing its own fragmentation channels that result in the generation of these NIs. In the case of $[M-X]^-$ NIs, one of them could be the σ*(OX) shape resonance. However, this conclusion would completely cancel a previously proposed mechanism [27] for the formation of $[M-X]^-$ NIs at 1.2–1.3 eV via a broad σ*(OX) shape resonance since the same resonance cannot decay twice at two different energies into the same type of fragment ions. In order to confirm the suggestion that a σ*(OX) shape resonance appears only at ca. 3 eV to produce the $[M-X]^-$ NIs, it is necessary to prove that other possible mechanisms, i.e., electronically excited Feshbach resonances are not involved.

The energy range 3–4.5 eV is typical for the lowest triplet and singlet excited states of simple compounds comprising carbonyl groups, C=O, such as formaldehyde [28] and acetone [29]. Within the framework of molecular orbital theory, these transitions are associated with excitation of an electron from the lone-pair of the carbonyl oxygen to an antibonding π^*_{OO} orbital. These excitations in compounds having the carboxyl group, C(O)OH, like formic and acetic acids undergo significant blue-shifts with energies ranging to ∼6 eV for the vertical and ∼5 eV for the adiabatic transitions [30]. Remarkably for methyl formate, the energy for the lowest singlet excitation is not much, if different at all [30]. A quick analysis of the singlet–triplet splitting for different carbonyl and carboxyl group compounds shows that it varies within several tenths of electron volts for both adiabatic and vertical transitions: formaldehyde (0.4–0.5 eV) [28a]; acetaldehyde (0.18–0.25 eV) [31]; formic acid (ca. 0.17 eV) [32]. We are not aware of similar gas phase data on amino acids having been reported. Direct comparison with available condensed-phase absorption spectra is hardly valid since interactions with the surrounding medium can affect both the energy and the order of transitions. Accordingly, high-quality calculations of the gas phase singlet transitions in amino acids were performed using a hierarchy of coupled cluster methods [33]. In those studies excellent agreement with experimental data considered reliable was reported. The lowest $n_O \rightarrow \pi^*_{CO}$ singlet transitions were predicted to require 5.88 eV energy in the case of Gly and 5.96 eV in the case of Ala, i.e., both being very close to that of carboxylic acids. Unfortunately, Osted et al. [33] did not report on the energies of the corresponding triplet transitions, but since singlet–triplet energy splitting for the related carboxylic acids does not exceed ∼0.5 eV, it is hardly likely that triplet states in amino acids are much lower in energy than the singlet transitions. These facts taken together argue against the resonances near 3 eV being a result of electronically excited Feshbach resonances with the triplet state of the neutral molecules as parent states. Furthermore, the electron affinity for such a scenario would be ∼2 eV which when recalling that the Gly ground state has a negative electron affinity and a dipole-bound state that provides positive electron affinity but not greater than 100 meV [20], makes this concept wholly untenable.

Therefore, it is proposed that the three types of NIs observed in Gly and its esters near 3–3.5 eV are generated from σ* shape resonance(s). $[M-X]^-$ NIs associated with the σ*(OX) shape resonances have already been discussed in part above; the only issue not considered so far is the increasing intensity of these ions near 3 eV for esters proceeding from Met to *t*-Bu. It is interesting that the only Gly conformer dipole moment that steadily increases with increasing size of the alkyl group of the ester functionality, is the III_p conformer (Table 2). The positive end of the dipole in III_p is directed towards the OX-group of the molecule and therefore, one may expect coupling between dipole-supported and valence σ*(OX) NI states as they both have A' symmetry. As already noted, such an interaction precludes crossing of two states of the same symmetry with the result that two adiabatic states above and below the crossing points of the diabatic states are generated (Fig. 4). However, because of the

massiveness of the alkyl radicals (X) of the esters, tunneling from the dipole-bound part of the lower adiabatic surface to the repulsive valence state is not possible in contrast to that that is observed for the hydrogen atom in Gly. On the other hand, the upper adiabatic surface is bounding at some O–X distances and since the energy of the σ*(OX) near 3 eV in Gly is lower than the thermochemical O–X bond dissociation energy (BDE), these NIs can only decay through electron autodetachment. For Gly Me-ester, the energy of σ*(OX) resonance is close to or even slightly higher than the BDE for OX and as the ester functionality increases in size, the BDE (OX) becomes lower than the energy of the σ*(OX) shape resonance and fragmentation with formation of $[M-X]^-$ in Gly esters near 3 eV becomes possible. The relative intensity of $[M-X]^-$ at 3.5 eV for the *i*-Pr ester is greater than for the *t*-Bu ester, because of the higher temperature used in the earlier experiments in which the molar concentration of the III_p conformer was higher. To stress the importance of the proposed coupling mechanism of two NI states, it is noted that the energy of the σ*(OX) shape resonance is higher than the thermochemical threshold for the production of $[M-X]^-$ in both Gly and its esters. However, fragmentation becomes possible only when fast electron autodetachment is suppressed by creation of a temporal bound NI state thereby providing an opportunity for rearrangement to occur (see below), or when the resonance energy is higher than the BDE of the neutral molecule. Suppression of electron autodetachment in these NIs presumes effective energy exchange between vibrational modes; a situation that is more complex than in the case of the one-dimensional model described for the Gly-base compounds (Fig. 4) and some other molecules [18c,d].

Additional support for more than a one-dimensional representation of these complex NI states is provided by the observation of one more fragmentation channel from the upper adiabatic potential energy surface that results in the formation of OX^- near 3 eV. Intensity changes for these ions for the four esters were similar to that of the $[M-X]^-$ NIs. The σ*(OX) orbital that is associated with the corresponding shape resonance and that is involved in coupling with the dipole-bound NI state, has a contribution on the OX-group as well as on the C–OX bond, only to a much lower extent. That is why OX^- NIs were observed with lower intensity than the $[M-X]^-$ NIs. It is also noted that OX^- from Gly is not observed in the energy range near 3 eV although the thermochemical threshold for the process is estimated to be 2.74 eV for I_p and 2.8 eV for III_p conformers. Here again the resonance energy is lower than the BDE for C–OX and since the upper adiabatic state is bound in the vicinity of the crossing point, fragmentation is suppressed.

The only NIs that were probably generated from the Gly upper adiabatic state were $COOX^-$. Thermochemical estimates indicate that the structure of these NIs at these electron energies is $HCOO^-$, not $COOH^-$. This means that generation of the ions requires rearrangement of the molecular structure and a bound adiabatic upper state serves as an effective mechanism against electron autodetachment. In esters, the restricted mobility of the heavier X-group prevents rearrangement and these ions are thus observed only at higher energies for the $COOX^-$ structure (Table 1).

$[M-H]^-$ NIs observed in esters slightly below 3 eV (Table 1) are probably associated with hydrogen-atom loss from the C_α-carbon. Indeed, taking into account the experimentally determined appearance energy (1.10 ± 0.05 eV) for the carboxylate anion [12] and the calculated energy differences between carboxylate, enolate and amide anions [34], the appearance energies should be 2.64 eV and 3.44 eV for the enolate and amide structures, respectively. The absence of these $[M-H]^-$ NIs in the energy range near 3 eV in Ala and Phe also favors this assignment. The $[M-H]^-$ NIs in this energy range are presumably formed from σ* shape resonances as suggested by the calculated σ^*_{N-H} virtual orbital energy (Table 2). With increasing ester group size, the wave function contribution to the C_α–H bond decreases and so does the relative intensity of the associated $[M-H]^-$ ion. The higher temperature did not affect the yield of these ions and therefore, these ions at this energy are mainly produced from the I_p conformer. It is probably the peculiarity of this shape resonance for the ion to survive electron autodetachment and instead to fragment. The relatively low energy of the process favors its survival.

The main significance of the resonances near 5–6 eV is that they produce all major NIs generated from Gly and its esters (Table 1). This energy range in amino acids according to Osted et al. [33] corresponds to two types of excitations, which are $n_O \rightarrow \pi^*_{CO}$ (~5.9 eV) and $n_N \rightarrow 3s$ (~6.3–6.4 eV). These neutral excited states could be parent states for the corresponding NIs that are formed via electronically excited Feshbach resonances. There are several σ* NI states in this energy range, one of which is σ^*_{C-OX} (Table 2). These σ* NI states are repulsive along some bonds and interaction of Feshbach resonances with these σ* states results in fragment NIs. Good spatial overlap of the σ^*_{C-OX} orbital and the excited $n_O \rightarrow \pi^*_{CO}$ state supports effective mixing for the corresponding shape and Feshbach resonances and the high yields of the OX^- NIs at 5.5–6 eV. Another consequence of the interaction between shape and Feshbach resonances is that the most characteristic NIs (Table 2) in Gly-based compounds are generated at 5–6 eV and these are associated with the carboxyl group. On the other hand, it is unclear why $COOX^-$ NIs in Gly and the Me ester are even more intense than the OX^- NIs, while the $COOX^-$ NIs become less intense the larger the ester group. The only transition that has nothing to do with the carboxyl group is the $n_N \rightarrow 3s$ transition associated with the amino group. The corresponding core-excited Feshbach resonance can be involved in the production of $[M-NH_2]^-$ at 5–5.5 eV. Feshbach resonances act as "doorways" [18] for repulsive NI states associated with σ* shape resonances. The σ* resonances themselves are probably very short-lived at these energies and without involvement of Feshbach resonances they can hardly support fragmentation of NIs of Gly and its esters.

The lowest Rydberg state in Gly is that involving the $n_N \rightarrow 3s$ transition. Other Rydberg states, associated with electron excitation from nitrogen and oxygen lone-pairs and $\pi_{C=O}$, can be considered as parent states for the high-energy resonances (≥7 eV) of Gly and its esters. Of the valence state transitions, π–π* excitation also occurs in this energy range. Osted et al. [33] predicted that these transitions in Gly require energy of

Table 3
Resonant electron capture mass spectra of alanine, $H_2NCHRC(O)OX$[a], (X = H) and its methyl (X = Me), ethyl (X = Et), and *t*-butyl (X = *t*-Bu) esters

Ions	X = H			X = Me			X = Et			X = *t*-Bu		
	m/*z*	*I*, % (E_m, eV)	I_{int}	*m*/*z*	*I*, % (E_m, eV)	I_{int}	*m*/*z*	*I*, % (E_m, eV)	I_{int}	*m*/*z*	*I*, % (E_m, eV)	I_{int}
$[M-H]^-$	88	56 (5–7)[b]	90	103	5 (≈5.5)	2	116	4.5 (≈5.5)	3.9	144	14 (≈5.1)	4.8
$[M-X]^-$	88	4375 (1.2)	3867	88	20 (≈1.2-1.3)[c] 6 (≈1.8-2.5)[b] 10 (≈9.5)	9	88	121 (≈3.3)[d] 125 (≈9)	217	88	213 (≈3.5)[e] 185 (≈9.3)	400
$[M-NH_2]^-$	73	100 (1.55)	45	87	7 (≈2) 6 (≈5)	3	101	6.3 (≈2) 4.5 (≈5.4)	4.3	129	10 (≈1.8) 2 (4–7)[b] 2 (8–10)[b]	4.4
$[M-OX]^-$	72	56 (1.5)[f] 10 (5) 20 (9)	47	72	2 (7–9)[b]	2	72	1.8 (4–6)[b] 2.5 (7–10)[b]	3.5	72	3.6 (4–6)[b] 2 (7–10)[b]	4
$[M-H-HOX]^-$	70	23 (≈5.5) 40 (8.5)	22	70	16 (≈5.5) 46 (≈8.5)	25	70	18 (≈5.5) 50 (≈8.8)	43	70	26 (≈5.5) 49 (≈8.8)	48
$COOX^-$	45	58 (2.3) 125 (5.7) 50 (9)	120	59	85 (5.5) 46 (≈7.5)	55	73	40 (≈5.6) 18 (≈7.5)	24	101	1.3 (4–8)[b]	0.6
OX^-	17	100 (5.5) 90 (6.7) 71 (8.5)	100	31	10 (≈3) 100 (≈5.6) 78 (≈7.3) 65 (≈9)	100	45	7 (≈ 3.1) 100 (≈5.6) 45 (≈7.2) 30 (≈9.5)	100	73	<2 (≈3) 100 (≈5.5)[e] 30 (≈9)	100

[a] R = CH_3.
[b] Precise determination of resonance maxima was not possible.
[c] These ions at low (1.2–1.3 eV) energy are supposed to be $[M-H]^-$ ions from underivatized alanine that may be present as an impurity.
[d] The effective yield curve of these ions is very wide and a determination of contributions from the resonance states near 2 and 5 eV is not possible.
[e] The effective yield curve of these ions is very wide and determination of possible contribution from the resonance state near 7 eV is impossible.
[f] By analogy with glycine, these NIs at 1.5 eV are supposed to be $[M-NH_3]^-$ rather than $[M-OX]^-$.

7.2–8.8 eV. Weiss and Krauss [35] showed that many Rydberg states possess positive electron affinity in the Franck–Condon region. Corresponding core-excited Feshbach resonances can be described as two electrons in the field of a positive ion, which in turn is formed by removing an electron from the highest occupied molecular orbital n_N, n_O, or $\pi_{C=O}$. Positive electron affinities of Rydberg states prevent core-excited Feshbach resonances from undergoing fast electron autodetachment, thus allowing survival of the NIs until fragmentation via mixing with a repulsive NI state can take place.

4.2. Alanine esters

The electronic structures of the two simplest amino acids are very similar and therefore, dramatic differences in gas phase resonance electron capture reaction between Ala and Gly are expected to be unlikely. Indeed, resonant electron capture spectra of Ala and its esters (Table 3; Fig. 6) and that of Gly both carried out under the same conditions are practically identical. Quantum chemical calculations (Table 4) of Ala conformers and that of its esters also showed similar results with Gly-based species. The only apparent difference was the absence of $[M-H]^-$ NIs in the energy range near 3 eV in the Ala spectra in comparison to that of Gly. As suggested above, formation of these NIs in Gly is most likely associated with hydrogen-atom loss from the C_α-carbon. Substitution of one of the hydrogen atoms at the C_α-carbon with the methyl group in Ala affected this fragmentation channel dramatically. Quantum chemical calculations predicted that the σ^*_{N-H} molecular orbital in Ala has only a small contribution on the C_α-carbon in contrast to that in Gly. Since the rest of the fragmentation channels showed no apparent changes, all mechanistic considerations apply equally well to Gly and Ala and their esters.

4.3. Phenylalanine esters

The main difference in resonant electron capture spectra of Phe and its esters with respect to the aliphatic counterparts is the observation of fragmentations associated with the side chain, R (Table 5). R^- ions were observed in underivatized Phe both at low (1.4 eV) and high (6.4 eV) energies, whereas $[M-R]^-$ were evident only at low energies. For the Phe esters, R^- ions were registered only at high energies and the $[M-R]^-$ ions only at low energies. Observation of $[M-R]^-$ at high energies with very low intensity in the case of *i*-Pr ester is probably associated with some conformers that were not sufficiently abundant at low temperatures. It was suggested earlier [12] that π^* shape resonances associated with the phenyl ring of Phe produce these ions at low energies (Table 6). Since Phe requires a higher temperature for volatilization in comparison to Gly and Ala, contribution

Table 4
Results of quantum chemical calculations of conformers of Ala (X = H) and its esters (X = Me, Et, and *t*-Bu) on the base of HF 6-31G* level of theory; E_{rel} is the total energy for different conformers with respect to that of I_p conformer; μ dipole moment; $E[\pi^*_{OO}]$ is energy of corresponding vacant molecular orbital scaled according to equations from Ref. [21][a]

	Conformers				
	I_p	II_n	III_p	IV_n	V_n
X = H					
E_{rel} (kcal/mol)	0	2.54	2.58	1.87	1.48
μ (D)	1.4	5.55	1.67	2.33	1.79
$E[\pi^*_{OO}]$ (eV)	1.83	1.94	1.78	1.91	1.82
	Conformers				
	I_p	II_n[b]	III_p	IV_n	V_n
X = Me					
E_{rel} (kcal/mol)	0	14.44	2.05	1.79	1.48
μ (D)	1.96	4.79	1.88	2.34	2.27
$E[\pi^*_{OO}]$ (eV)	1.91	1.80	2.27	1.98	1.9
X = Et					
E_{rel} (kcal/mol)	0	14.26	2.63	1.79	1.49
μ (D)	2.14	4.67	2.43	2.44	2.44
$E[\pi^*_{OO}]$ (eV)	1.94	1.83	1.87	2.02	1.93
	Conformers				
	I_p	II_n[b,c]	III_p	IV_n	V_n
X = *t*-Bu					
E_{rel} (kcal/mol)	0	34.12[c]	2.33	2.03	1.5
μ (D)	2.24	6.05	2.5	2.48	2.49
$E[\pi^*_{OO}]$ (eV)	1.96	1.80	1.93	1.91	1.95

[a] See the footnote (a) to Table 2.
[b] Because of the non-planar structures, many orbitals mutually mixed and it was difficult to identify some of them.
[c] Geometry of this conformer was taken from the PM3 calculations, since optimization on the basis of HF 6-31G* resulted in geometry of the IV conformer.

Table 5
Resonant electron capture mass spectra of phenylalanine, $H_2NCHRC(O)OX$[a], (X = H) and its methyl (X = Me), ethyl (X = Et), isopropyl (X = *i*-Pr), and *t*-butyl (X = *t*-Bu) esters

Ions	X = H[b]			X = Me			X = Et			X = *i*-Pr[c]			X = *t*-Bu		
	m/z	*I*,% (E_m, eV)	I_{int}	*m/z*	*I*, % (E_m, eV)	I_{int}	*m/z*	*I*, % (E_m, eV)	I_{int}	*m/z*	*I*, % (E_m, eV)	I_{int}	*m/z*	*I*, % (E_m, eV)	I_{int}
$[M-H]^-$	164	6 (5–7)[d]	63	178	28 (≈5.5) 16 (≈8.4)	22	192	28 (≈5.5) 10 (≈8.5)	22	206	≈8(5–6)[d]	4	220	23 (≈5.5) <10 (7–9)[d]	22
$[M-X]^-$	164	1060 (1.16)	1065	164	<5 (≈1.2)[e] 5.3 (≈1.9) 7.4 (≈10)	9	164	128 (≈3.2)[f] 119 (≈9.2)	204	164	277 (≈3.5) 86 (8–10)[d]	370	164	130 (3.6) 154 (≈9.3)	222
$[M-NH_2]^-$	149	43 (1.71) 14 (5.5)	29	163	6 (≈1.9) 8.5 (≈5.5)	7	177	10 (≈1.8) 15 (≈5.5)	12	191	11 (1–2)[d] <1 (5–6)[d]	11	205	<7 (1–2)[d] <7 (4–10)[d]	6
$[M-OX]^-$	148	14 (5.3)	15	148	2.6 (5–7)[d] 4.7 (8–10)[d]	3	148	5 (8–10)[d]	6	148	10 (6–10)[d]	11	148	<7 (4–10)[d]	9
$[M-H-HOX]^-$	146	7 (6)	8	146	45 (≈5.9) 23 (≈8)	39	146	42 (≈5.9) 28 (≈8.5)	39	146	14 (5.5)	15	146	54 (≈5.8) ≈25 (8-9)[d]	47
$COOX^-$	45	21 (6.5)	17	59	34 (≈7.6) 26 (≈8.8)	28	73	23 (7–9)[d]	16	87	<1 (7–8)[d]	7	101	<7 (7–10)[d]	3
OX^-	17	100 (6)	100	31	100 (≈6.5)[g]	100	45	100 (≈6.5) 28 (≈8–9)[d]	100	59	100 (≈6.5) ≈30 (7–9)[d]	100	73	100 (≈6.3) ≈30 (7–9)[d]	100
R^-	91	14 (1.4) 36 (6.4)	26	91	50 (≈6.4)[h]	59	91	36 (≈6.5)[h]	44	91	40 (≈6.5)[h]	37	91	38 (5–7)[d]	44
$[M-R]^-$	74	143 (1.45)	130	88	11 (≈1.8)	9	102	19 (1.5–1.7)[d]	8	116	39 (1–2)[d] <1 (5–6)[d]	30	130	23 (1–2)[d]	13

[a] $R = CH_2\text{-}C_6H_5$.
[b] These data have been taken from Ref. [12].
[c] Experimental conditions similar to that of Ref. [12] (high temperature) have been used to record spectra of this compound.
[d] Precise determination of resonance maxima was not possible.
[e] Ions at low (≈1.2 eV) energy are supposed to be $[M-H]^-$ ions from underivatized phenylalanine that may present as impurity.
[f] The effective yield curve of these ions is very wide and determination of possible contribution from the resonance state in the vicinity of 2 eV is impossible.
[g] The effective yield curve of these ions is very wide and a determination of their contribution from the resonance states at energy lower than 5 eV and higher than 8 eV was not possible.
[h] There is substantial contribution to the effective yield curve in the energy range 7–11 eV but strong interference of different resonance states producing these ions makes it impossible to resolve these states.

of $[M-H]^-$ NIs from underivatized Phe in the resonant electron capture spectra of Phe esters was minimal (Fig. 7). Indeed, only Phe Me ester showed ions with *m/z* 164 at 1.2 eV and that with only relatively low abundance. In analogy with Ala, Phe, and its esters did not form $[M-H]^-$ NIs near 3 eV because one of the hydrogen atoms on the C_α-carbon was replaced by the side chain. As in the case of Ala, such substitution resulted in a dramatic decrease in the contribution of the σ^*_{N-H} molecular orbital on the C_α-carbon. OX^- NIs from Phe and its esters were not observed from resonances near 3 eV in contrast to those observed from Gly and Ala. The problem may be due to the changing character of the wave function in σ^*_{OX} orbital. Indeed, calculations using HF 6-31G* level of theory predicted a decreased contribution of this orbital on the C–OX bond in favor of the OX-bond as the ester groups increased in size. For Phe this was already the case for the underivatized amino acid; the esters did not change this scenario. The rest of the resonant electron capture spectra of Phe and its esters were similar to that of the Gly based materials. Therefore, all mechanistic considerations apply equally well to both Gly and Ala. The problem may be due to the changing character of the wave function in σ^*_{OX} orbital. Indeed, calculations using HF 6-31G* level of theory predicted a decreased contribution of this orbital on the C–OX bond in favor of the OX-bond as the ester groups increased in size. For Phe this was already the case for the underivatized amino acid; the esters did not change this scenario. The rest of the resonant electron capture spectra of Phe and its esters were similar to that of the Gly based materials. Therefore, all mechanistic considerations apply equally well to both Gly and Phe and their esters.

Table 6
Results of quantum chemical calculations of conformers of Phe (X = H) and its esters (X = Me, Et, *i*-Pr, and *t*-Bu) on the base of HF 6-31G* level of theory: E_{rel} is the total energy for different conformers with respect to that of I_p conformer; μ dipole moment; $E[\pi^*_{OO}]$, $E[\pi^*(Ph(a_2))]$ $E[\pi^*(Ph(b_1))]$[a] are energies of corresponding vacant molecular orbitals scaled according to equations from Ref. [21][b]

	Conformers				
	I_p	II_n	III_p	IV_n	V_n
X = H					
E_{rel} (kcal/mol)	0	1.37	0.85	2.85	3.19
μ (D)	1.32	5.18	1.76	2.44	2.37
$E[\pi^*(Ph(b_1))]$ (eV)	0.96	0.83	0.97	0.9	0.87
$E[\pi^*(Ph(a_2))]$ (eV)	0.94	0.85	0.97	0.91	0.88
$E[\sigma^*_{OO}]$ (eV)	1.91	1.7	1.82	1.97	1.95
	Conformers				
	I_p	II_n[c]	III_p	IV_n	V_n
X = Me					
E_{rel} (kcal/mol)	0	12.74	0.77	2.85	6.27
μ (D)	1.85	4.32	2.29	2.48	2.18
$E[\pi^*(Ph(b_1))]$ (eV)	0.99	0.98	0.99	0.92	0.88
$E[\pi^*(Ph(a_2))]$ (eV)	0.97	1.05	0.99	0.94	0.92
$E[\sigma^*_{OO}]$ (eV)	1.96	1.66	1.91	2.03	1.88
X = Et					
E_{rel} (kcal/mol)	0	13.65	0.75	2.85	2.87
μ (D)	2.02	4.18	2.46	2.57	2.52
$E[\pi^*(Ph(b_1))]$ (eV)	0.98	0.99	0.99	0.93	0.88
$E[\pi^*(Ph(a_2))]$ (eV)	0.99	1.06	1.00	0.95	0.91
$E[\sigma^*_{OO}]$ (eV)	2.01	1.65	1.95	2.07	2.07
X = *i*-Pr					
E_{rel} (kcal/mol)	0	12.67	3.31	2.72	5.63
μ (D)	2.01	4.14	2.42	2.45	2.2
$E[\pi^*(Ph(b_1))]$ (eV)	0.99	0.98	1.00	0.94	0.9
$E[\pi^*(Ph(a_2))]$ (eV)	1.00	1.06	1.01	0.96	0.92
$E[\sigma^*_{OO}]$ (eV)	2.02	1.66	1.92	2.06	2.02
	Conformers				
	I_p	II_n[c,d]	III_p	IV_n	V_n
X = *t*-Bu					
E_{rel} (kcal/mol)	0	38.11	0.47	2.83	2.71
μ (D)	2.11	4.28	2.52	2.32	2.29
$E[\pi^*(Ph(b_1))]$ (eV)	1.00	0.86	1.0	0.97	0.9
$E[\pi^*(Ph(a_2))]$ (eV)	1.01	0.87	1.0	0.99	0.92
$E[\sigma^*_{OO}]$ (eV)	1.99	1.38	1.95	2.05	2.05

[a] Ph means that these orbitals are mainly located on the phenyl group of the side chain.
[b] See the footnote (a) to Table 2.
[c] Because of the non-planar structures, many orbitals mutually mixed and it was difficult to identify some of them.
[d] Geometry of this conformer was taken from the PM3 calculations, since optimization on the basis of HF 6-31G* resulted into geometry of the IV conformer.

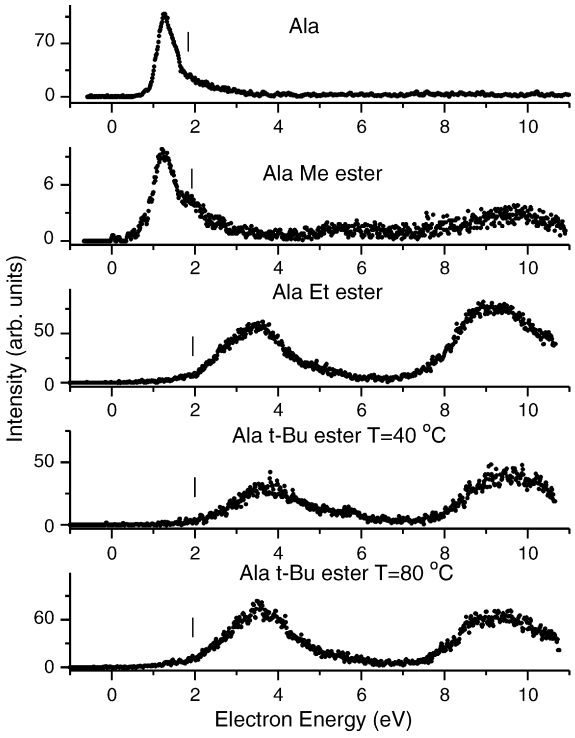

Fig. 6. Effective yield curves of $[M-X]^-$ NIs from Ala and its esters. The vertical bars indicate positions of π^*_{OO} shape resonances determined either from calculations (esters; see also Table 4) or taken from Ref. [21] (Ala). Effective yield curves of $[M-X]^-$ negative ions from *t*-Bu ester have been recorded at two different temperatures.

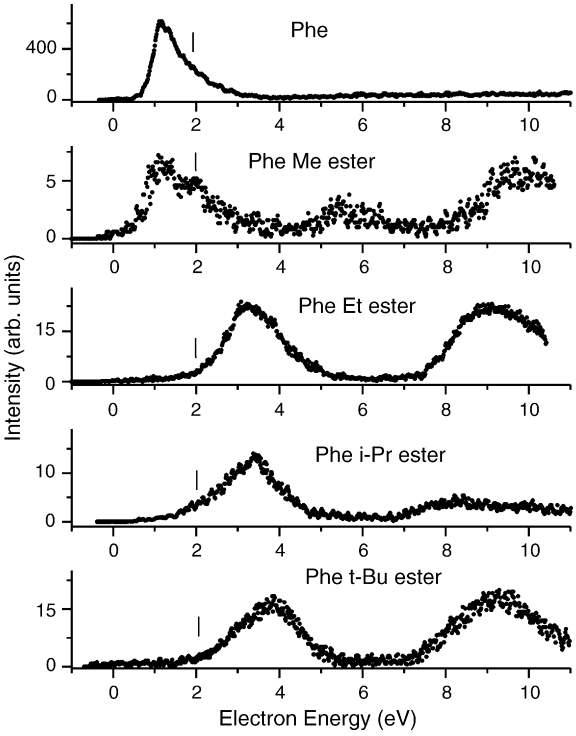

Fig. 7. Effective yield curves of $[M-X]^-$ NIs from Phe and its esters. The vertical bars indicate positions of π^*_{OO} shape resonances determined either from calculations (esters; see also Table 6) or taken from Ref. [21] (Phe).

5. Conclusions

The most efficient and characteristic decay channels of the ester NI resonances are those associated with the production of the C-terminal fragment NIs, namely $[M-X]^-$, $COOX^-$, and OX^- (X is Me, Et, *i*-Pr, or *t*-Bu). Although slight variations in resonance electron energies and relative intensities were observed, the effective yield curves for $COOX^-$ and OX^- NIs as functions of electron energy appear at 5.5–6 and 7–10 eV and are similar in most respects for all three amino acids and their esters. Some Gly and Ala esters form OX^- NIs at 3–3.3 eV as well *albeit* with low efficiency. In contrast, generation of $[M-X]^-$ NIs has been found to be very efficient in the low-energy range achieving maximum intensity for *i*-Pr and *t*-Bu esters for all amino acids studied here. Generation of these NIs is easily rationalized by a model that involve coupling of two NI states one of which is a common "chemical" or valence state and the other a dipole-supported or dipole-bound state of the same symmetry. This coupling precludes crossing of these two states and instead the creation of two adiabatic states. The upper state is bound within some values of a reaction coordinate and therefore, fragmentation occurs when the resonance energy exceeds the thermochemical BDE for the neutral molecule. Other ions, like $[M-H]^-$ ions can be generated at the lower adiabatic state via tunneling through the barrier that separates a dipole-supported minimum and repulsive valence state. The present data do not support the earlier proposed mechanism for generation of these $[M-H]^-$ NIs at energies <1.5 eV through π^*_{OO} shape resonances. This mechanism applies when resonant energies are >1.5 eV. States decaying into fragment NIs in the energy range 5–6 eV are supposed to be electronically excited Feshbach resonances associated with n–π* singlet excited and n–3s Rydberg excited states of the corresponding neutral molecules. Since the carboxylate group is involved in such electronic excitations, the C-terminal ions are the most abundant species observed. NIs produced at energies >7 eV involve core-excited Feshbach resonances. Comparison of high and low temperature experiments revealed the difference in amino acid conformer concentrations in the gas phase is a function of temperature. The II_n conformers, played a very important role in the resonance electron capture spectrum for the underivatized amino acids, but these contributed little if any in the case of resonant electron capture spectra of the esters. In general, quantum chemical calculations showed that esterification of amino acids had only a limited influence on their electronic structures. However, the differences in the thermochemical characteristics of underivatized amino acids and their esters resulting from different masses of the departing particles, had a major impact on the fragmentation mechanisms in both cases. Methylation in comparison to esterification by larger alkyl groups caused the least change in fragmentation behavior. During preparation of this manuscript, it was learned that Burrow and coworkers [36] have also noted the difference between the electron transmission and dissociative electron attachment spectra of amino acids in the low energy range 1.2–1.3 eV which indicated to these authors as well that π^*_{OO} shape resonances apparently are not involved in fragmentation of these compounds to produce $[M-H]^-$ NIs.

Acknowledgements

This project was supported by individual NIH research grants ES09536 and ES10338, and by the W.M. Keck foundation award. This publication was made possible in part by grant number P30 ES00210 from the National Institute of Environmental Health Sciences, NIH. The authors wish to acknowledge the Mass Spectrometry Facility of the Environmental Health Sciences Center at Oregon State University. We would like to express our gratitude to Prof. Paul Burrow for sending his manuscript [36] before submission and for bringing to the authors' attention the work from the Allan group [27] and contributions on photoelectron spectroscopy of negatively charged Gly clusters [19,20].

References

[1] L. Sanche, Mass Spectrom. Rev. 21 (2002) 349.
[2] M.V. Muftakhov, Y.V. Vasil'ev, V.A. Mazunov, Rapid Commun. Mass Spectrom. 13 (1999) 1104.
[3] S. Gohlke, A. Rosa, E. Illenberger, F. Brüning, M.A. Huels, J. Chem. Phys. 116 (2002) 10164.
[4] S. Ptasinska, S. Denifl, A. Abedi, P. Scheier, T.D. Märk, Anal. Bioanal. Chem. 377 (2003) 1115.
[5] S. Ptasińska, S. Denifl, P. Candori, S. Matejcik, P. Scheier, T.D. Märk, Chem. Phys. Lett. 403 (2005) 107.
[6] H. Abdoul-Carime, S. Gohlke, E. Illenberger, Phys. Chem. Chem. Phys. 6 (2004) 161.
[7] H. Abdoul-Carime, E. Illenberger, Chem. Phys. Lett. 397 (2004) 309.
[8] H. Abdoul-Carime, S. Gohlke, E. Illenberger, Chem. Phys. Lett. 402 (2005) 497.
[9] H. Abdoul-Carime, S. Gohlke, E. Illenberger, J. Am. Chem. Soc. 126 (2004) 12158.
[10] P. Papp, J. Urban, S. Matejčik, M. Stano, O. Ingolfsson, J. Chem. Phys. 125 (2006) 204301.
[11] W. Vetter, in: G.R. Waller (Ed.), Biochemical Applications of Mass Spectrometry, Willer-Interscience, New York, 1972, p. 387.
[12] Y.V. Vasil'ev, B. Figard, V.G. Voinov, D.F. Barofsky, M.L. Deinzer, J. Am. Chem. Soc. 128 (2006) 5506.
[13] Y.V. Vasil'ev, B. Figard, M.L. Deinzer, in: M.L. Gross, R.M. Caprioli (Eds.), Encyclopedia of Mass Spectrometry: Molecular Ionization, vol. 6, Elesevier, New York, NY, 2007, p. 295.
[14] D.T. Nguyen, A.C. Scheiner, J.W. Andzelm, S. Sirois, D.R. Salahub, A.T. Hagler, J. Comput. Chem. 18 (1997) 1609.
[15] M. Gutowski, P. Skurski, J. Simons, J. Am. Chem. Soc. 122 (2000) 10159.
[16] O.H. Crawford, Mol. Phys. 20 (1971) 585.
[17] W.R. Garrett, J. Chem. Phys. 77 (1982) 3666.
[18] (a) P.D. Burrow, G.A. Gallup, A.M. Scheer, S. Denifl, S. Ptasinska, T. Märk, P. Scheier, J. Chem. Phys. 124 (2006) 124310;
(b) K. Aflatooni, A.M. Scheer, P.D. Burrow, J. Chem. Phys. 125 (2006) 054301;
(c) T. Sommerfeld, J. Phys. Chem. A 108 (2004) 9150;
(d) T. Sommerfeld, Phys. Chem. Chem. Phys. 4 (2002) 2511.
[19] S. Xu, M. Nilles, K.H. Bowen Jr., J. Chem. Phys. 119 (2003) 10696.
[20] E.G. Diken, N.I. Hammer, M.J. Johnson, J. Chem. Phys. 120 (2004) 9899.
[21] K. Aflatooni, B. Hitt, G.A. Gallup, P.D. Burrow, J. Chem. Phys. 115 (2001) 6489.
[22] V.G. Voinov, Y.V. Vasil'ev, H. Ji, B. Figard, J. Morré, T.F. Egan, D.F. Barofsky, M.L. Deinzer, Anal. Chem. 76 (2004) 2951.
[23] A.G. Császár, J. Am. Chem. Soc. 114 (1992) 9568.
[24] D. Voigt, J. Schmidt, Biomed. Mass Spectrom. 5 (1978) 44.
[25] F. Huisken, O. Werhahn, A.Yu. Ivanov, S.A. Krasnokutski, J. Chem. Phys. 111 (1999) 2978.
[26] Y.V. Vasil'ev, M.V. Muftakhov, G.M. Tuimedov, R.V. Khatymov, R.R. Abzalimov, V.A. Mazunov, T. Drewello, Int. J. Mass Spectrom. 205 (2001) 119.
[27] M. Allan, J. Phys. B: At. Mol. Opt. Phys. 39 (2006) 2939.
[28] (a) A. Chutjian, J. Chem. Phys. 61 (1974) 4279;
(b) S.D. Peyerimhoff, R.J. Buenker, W.E. Kammer, H. Hsu, Chem. Phys. Lett. 8 (1971) 129.
[29] (a) W.M.St. John III, R.C. Estler, J.P. Doering, J. Chem. Phys. 61 (1974) 763;
(b) B. Hess, P.J. Bruna, R.J. Buenker, S.D. Peyerimhoff, Chem. Phys. 18 (1976) 267.
[30] E. Barnes, W.T. Simpson, J. Chem. Phys. 39 (1963) 670;
P. Hintze, S. Aloisio, V. Vaida, Chem. Phys. Lett. 343 (2001) 159.
[31] M. Allan, J. Electron Spectrosc. Relat. Phenom. 48 (1989) 219.
[32] H. Su, Y. He, F. Kong, W. Fang, R. Liu, J. Chem. Phys. 113 (2000) 1891.
[33] A. Osted, J. Kongsted, O. Christiansen, J. Phys. Chem. A 109 (2005) 1430.
[34] R.A.J. O'Hair, S. Blanksby, M. Styles, J.H. Bowie, Int. J. Mass Spectrom. 182/183 (1999) 203.
[35] A.W. Weiss, M. Krauss, J. Chem. Phys. 52 (1970) 4363.
[36] A.M. Scheer, P. Mozejko, G.A. Gallup, P.D. Burrow, J. Chem. Phys. 126 (2007) 174301.